Splitting of the excitonic peak in quantum wells with interfacial roughness

Hervé Castella
Department of Physics, Ohio State University, 174 West 18th Avenue, Columbus, Ohio 43210-1106
and Max-Planck-Institut für Physik Komplexer Systeme, Nöthnitzer Strasse 38, D-01187 Dresden, Germany

John W. Wilkins
Department of Physics, Ohio State University, 174 West 18th Avenue, Columbus, Ohio 43210-1106
(Received 10 August 1998)

Excitons in a quantum well depend on the interfacial roughness resulting from its growth. The interface is characterized by islands of size ξ separated by one monolayer steps across which the confining potential decreases by V_0 for wider wells. A natural length is the localization length $\xi_0=\pi\hbar/\sqrt{2MV_0}$ characterizing the minimum size island to confine an exciton. For small islands ($\xi<\xi_0$), the absorption spectrum has a single exciton peak. As the island size ξ exceeds the localization length ξ_0, the peak gradually splits into a doublet. Generally the spectra exhibit the following features: (1) the shape is very sensitive to ξ/ξ_0 and depends only weakly on the ratio of island size to exciton radius; (2) in the small island regime $\xi\ll\xi_0$, the asymmetric shape of the exciton peak is correctly described by a model of white-noise potential, except for the position of the peak which still depends on the correlation length of the disorder. [S0163-1829(98)06348-6]

I. INTRODUCTION

Optical and transport properties of narrow quantum well heterostructures are particularly sensitive to disorder at the interface between the different compounds forming the well and the barrier.[1] Local fluctuations of the well thickness produce an interfacial roughness that hinders the transport of charge carriers in the well or that pins excitons. The quality of the heterostructure can be improved by interrupting the growth process at the interfaces.[2] The atoms deposited on the surface diffuse during the interruption and form large smooth islands separated by one-monolayer steps. The size of the islands depends on both the interruption time and the temperature of the substrate.[3]

The interface roughness has been studied experimentally with different techniques such as photoluminescence, transmission electron microscopy, cathodoluminescence, and scanning tunneling microscopy.[1,4–6] In $GaAs/Al_xGa_{1-x}As$ quantum wells, islands of several μm in size have been directly observed by cathodoluminescence.[5] The photoluminescence spectrum is very sensitive to the size of the islands with an exciton line splitting for large-enough islands.[1,6,7] The interfacial roughness also plays an important role in resonant Rayleigh scattering in quantum wells.[8]

Theoretical studies of the photoluminescence have focused on the regime of small island size.[9–11] The rapid fluctuations of the interface are averaged by the relative motion of electron and hole producing for the exciton center of mass an effective potential that is smooth on the scale of the exciton radius. The absorption spectrum has a single asymmetric excitonic peak.

The present paper is a numerical study of the absorption spectrum in the presence of islands large enough to produce a splitting of the excitonic peak. Previous theoretical studies in this regime have been restricted to a broadening of delta functions by a Lorentzian whose width is estimated by statistical arguments.[12] Here, however, we use the quantum-mechanical approach of Ref. 9 to compute the absorption spectrum numerically for arbitrary island sizes.

The interfacial roughness is a particular type of disorder in two aspects: (a) it has long-range correlations which are essential for the splitting of the excitonic peak (see Sec. V) and (b) the disorder is discrete, that is, the potential changes abruptly at the edge of islands (see Sec. IV).

In close analogy to previous studies of the small islands regime,[9,11] the present paper emphasizes the role of the localization length $\xi_0=\pi\hbar/\sqrt{2MV_0}$ as the important length scale of the problem. This point of view contrasts with the usual experimental interpretation, which attributes the splitting to islands of size larger than the exciton radius.[1,6]

In Sec. II, the model is described and the main results are presented. Section III discusses the wave function of an exciton confined in a perfect quantum well and examines the importance of correlations between hole and electron in the direction perpendicular to the well. Section IV analyzes the statistical properties of the interface fluctuations and of the resulting potential for the exciton. Finally, Sec. V presents the calculations of the excitonic line shape in the absorption spectrum.

II. MODEL AND RESULTS

The model used here for excitons in quantum wells with interfacial roughness was introduced in Ref. 9 for the study of the alloy disorder in bulk semiconductors and applied by several authors to the problem of interfacial roughness.[10,11] While these studies have considered a rapidly fluctuating random potential, the present paper focuses on the regime where the interface consists of large smooth islands. This section presents the approximation for the exciton wave function in a perfect quantum well and then introduces the interface roughness. The main results of this work are summarized at the end of the section.

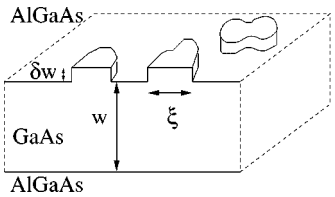

FIG. 1. View of the GaAs/Al_xGa_{1-x}As interface where steps of one monolayer in height form islands of typical size ξ. The steps at the interface correspond to changes δw in the thickness of the well of nominal width w.

A. Excitonic wave function in a perfect well

The wave function ψ is described by a quasi-two-dimensional approximation where the motion in the well and in the transverse direction are separated.[13] The electron and hole are assumed to be uncorrelated in the transverse direction z and to remain in the lowest bound state of the confining potential whose wave functions and energies for the electron and the hole are $\phi_0^e(z), \epsilon_0^e$ and $\phi_0^h(z), \epsilon_0^h$, respectively. The wave function in the plane of the well separates into a plane wave of total momentum $\vec{K}$ for the center of mass $\vec{R}$ and into a relative wave function $f(\vec{\rho})$ for the relative coordinate $\vec{\rho}$:

$$\psi(\vec{\rho},\vec{R},z_e,z_h)=e^{-i\vec{K}\cdot\vec{R}}f(\vec{\rho})\phi_0^e(z_e)\phi_0^h(z_h). \tag{1}$$

The relative wave function f with binding energy E_x satisfies a Schrödinger equation in an effective two-dimensional Coulomb potential $U_{eff}(\vec{\rho})$:

$$[-\nabla^2+U_{eff}(\vec{\rho})]f(\vec{\rho})=-E_x f(\vec{\rho}), \tag{2}$$

$$U_{eff}(\vec{\rho})=-2\int dz_e dz_h \frac{|\phi_0^e(z_e)|^2|\phi_0^h(z_h)|^2}{\sqrt{|\vec{\rho}|^2+(z_e-z_h)^2}}. \tag{3}$$

The effective Bohr radius $a_B=\epsilon\hbar^2/\pi\mu e^2$ and Rydberg $\mathcal{R}_y=\hbar^2/2\mu a_B^2$ in the bulk are the length and energy units where $\mu=m_e m_h/(m_e+m_h)$ is the reduced mass, m_e and m_h the electron and hole masses, and ϵ the dielectric constant. In these units, the exciton radius is defined as $a_x=1/\sqrt{E_x}$.

The total exciton energy in a perfect well consists of the single-particle confining energies, the exciton binding energy E_x and the center of mass kinetic energy: $E=\epsilon_0^e+\epsilon_0^h-E_x+\hbar^2K^2/2M$ with $M=m_e+m_h$. The next section will further discuss the validity of the quasi-two-dimensional approximation for narrow quantum wells.

B. Interfacial disorder

In a sample with growth interruption the interface consists of large smooth islands separated by steps of one monolayer in height. Figure 1 shows the islands of typical size ξ at the GaAs/Al_xGa_{1-x}As interface in a quantum well of nominal width w. The steps at the interface correspond to a change δw in the thickness of the well.

We consider the disorder at only one of the interface and further restrict the width fluctuations δw to either 0 or 1 in units of the monolayer height. The width fluctuations at different points of the interface are correlated over the typical island size ξ. Section IV and the Appendix A discuss the statistical distribution of islands and the numerical procedure, which generates such discrete random variables with long-range correlations.

C. Exciton wave function with disorder

The quasi-two-dimensional approximation for the exciton wave function is extended to the disordered well by choosing the transverse state $\phi_0^{e,h}$ as the ground state for a confining potential of nominal width w. Thus the electron and hole feel a potential drop $V_{e,h}$ when they sit in an island where the well thickness is $w+\delta w$; the potentials $V_{e,h}$ strongly depend on the nominal width since they are proportional to the density of electrons or holes within the excess monolayer: $V_{e,h}=\Delta_{e,h}\int_w^{w+\delta w}|\phi_0^{e,h}|^2dz$ with $\Delta_{e,h}$ being the valence- and conduction-band offsets.

While the potential fluctuations affect both the center of mass motion and the relative motion, we further simplify the model by fixing the relative wave function f to be the ground state for a perfect well of width w. This adiabatic approximation, valid only when the binding energy E_x exceeds the potential $V_0=V_e+V_h$, fails for narrow wells due to the increase of V_0.

D. Random potential

As a result of these approximations we are left with the problem of a single-particle subject to a random potential in two dimensions. The electron at position $\vec{r}_e=\vec{R}+m_h\vec{\rho}/M$ and the hole at $\vec{r}_h=\vec{R}-m_e\vec{\rho}/M$ feel the island potential $-V_e\delta w(\vec{r}_e)$ and $-V_h\delta w(\vec{r}_h)$, respectively. The random potential $V(\vec{R})$ for the center of mass is a convolution of the island potential with the relative wave function $f(\vec{\rho})$:

$$V(\vec{R})=-\int d^2\rho|f(\vec{\rho})|^2\left\{V_e\delta w\left(\vec{R}+\frac{m_h}{M}\vec{\rho}\right)+V_h\delta w\left(\vec{R}-\frac{m_e}{M}\vec{\rho}\right)\right\}. \tag{4}$$

The potential depends on the exciton radius a_x through the relative wave function and on the island size ξ via the correlation of δw. The kinetic energy introduces another length scale $\xi_0=\pi\hbar/\sqrt{2MV_0}$ that corresponds to the smallest island size that has a bound state.

The absorption spectrum at zero temperature $\alpha(E)$ is computed numerically from the eigenstates $\kappa_n(\vec{R})$ for the exciton center of mass in the presence of the disorder potential $V(\vec{R})$ and averaged over many random configurations:

$$\alpha(E)=\left\langle\sum_n\left|\int d^2R\kappa_n(\vec{R})\right|^2\delta(E-E_n)\right\rangle. \tag{5}$$

E. Results

Here we summarize the main results of this study which are presented in details in the next sections.

1. Quasi-two-dimensional approximation in a perfect well

For narrow quantum wells the confining potential allows only a single bound state, and the contribution to the exciton

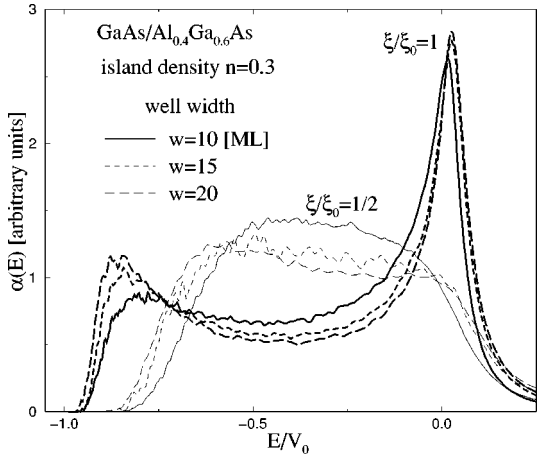

FIG. 2. Dependence of the absorption spectrum $\alpha(E)$ on normalized energy E/V_0 and on ratio of island size ξ to localization length ξ_0. The curves for a given ratio ξ/ξ_0 nearly coincide although they correspond to wells of different widths w and hence different ξ_0. The results for $\xi/\xi_0=1$ are shown as thick lines.

binding energy of excitations into unconfined states is evaluated perturbatively. In $GaAs/Al_{0.4}Ga_{0.6}As$ quantum wells, the two-dimensional approximation describes correctly the ground state of the exciton for widths larger than five ML where the coupling to unconfined states becomes important. The calculations are presented in Sec. III.

2. The strength and correlation length of the potential depend on ξ/a_x

In the small island regime $\xi/a_x \ll 1$ the relative motion of electron and hole reduces the intensity of the potential, which varies over a distance given by the exciton radius a_x. In the opposite regime, however, the potential is proportional to the width fluctuations $V(\vec{R})=-V_0\delta w(\vec{R})$ and has the same correlations as δw. Section IV discusses the statistical properties of the potential.

3. The absorption spectrum depends on E/V_0 and ξ/ξ_0

The absorption spectrum is very sensitive to the ratio of island size to localization length ξ/ξ_0, but depends only weakly on ξ/a_x and on the width w. Figure 2 shows the absorption spectrum as a function of normalized energy E/V_0 for wells that differ in w (and hence in ξ_0) but have a nearly constant a_x. For the range of w considered, nearly coincident curves correspond to the same value of ξ/ξ_0. The calculations of $\alpha(E)$ are discussed in Sec. V.

4. Gradual splitting of the excitonic peak

Figure 3 shows the splitting of the excitonic peak with increasing island size that occurs in the regime $1/4 \leqslant \xi/\xi_0 \leqslant 2$. Photoluminescence experiments show two excitonic peaks in samples prepared with growth interruption at the interface. The present study shows that the energy separation between the peaks depends on the size of islands in the intermediate regime $\xi \simeq \xi_0$.

5. White noise regime

The absorption spectrum in the small-island regime is correctly described by a model of white-noise potential. Figure 4 compares the numerical spectra to the analytical result of Ref. 11 for a δ-correlated potential. While the shape of the exciton peak agrees well with the numerical data, the position and peak value still depend on the correlation length. Section V shows how this discrepancy can be eliminated by a proper correction of the high-energy tail in the analytical result.

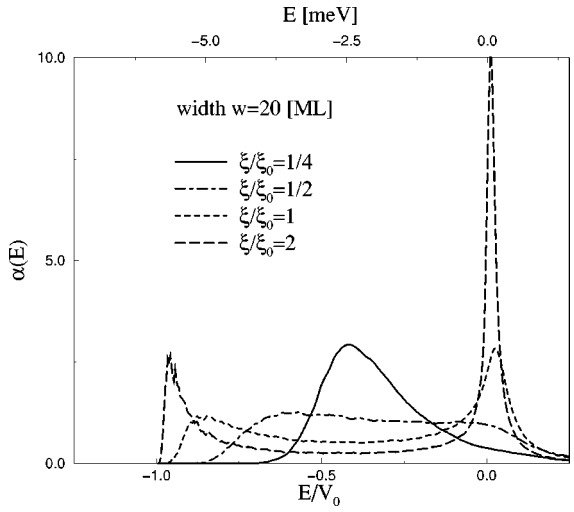

FIG. 3. Gradual splitting of the excitonic peak in the absorption spectrum $\alpha(E)$ with increasing ξ/ξ_0 for a well of 20 ML.

6. Localization properties

When the island size is sufficiently large to produce a splitting the exciton states contributing to the low-energy peak are localized within a single island while the states at higher energy extend over many islands. This result is consistent with recent near-field spectroscopy experiments which observed at low-energy sharp resonances attributed to quantum-dot levels.[14]

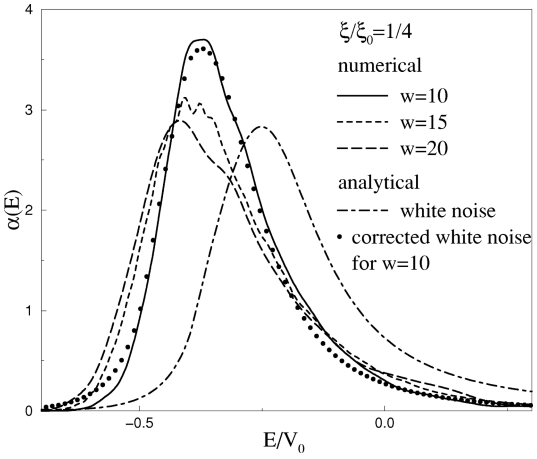

FIG. 4. Absorption spectrum $\alpha(E)$ in the small-island regime $\xi/\xi_0=1/4$. The numerical results for different widths differ in the position and the magnitude of the peak. The analytical formula for a white-noise potential from Ref. 11 reproduces the shape of the spectrum but has to be corrected for the finite-correlation length of the disorder to agree with the numerical data.

III. EXCITON IN A PERFECT WELL

This section addresses the validity of the quasi-two-dimensional approximation to the excitonic wave function in an ordered quantum well and perturbatively estimates the correction to the exciton binding energy.

The two-dimensional approximation in Eq. (1) retains only the ground-state wave functions of the confining potential for both hole and electron which are assumed to be uncorrelated in the transverse direction. This approximation has been studied in the literature by variational calculations that indicate correlations in the transverse direction to remain small for widths ranging from a few to 100 monolayers in $GaAs/Al_xGa_{1-x}As$ wells.[13] This section focuses on the narrow-well regime where the potential allows only a single shallow confined state. The remaining states are unconfined states and form a continuum; we assess their importance by a perturbative estimation of their contribution to the exciton binding energy.

The Coulomb potential U_c couples the ground-state wave function ψ within the two-dimensional approximation to excited states with transverse wave functions $\phi_n^e(z_e), \phi_m^h(z_h)$ and momentum $\vec{q}$ for the relative motion in the plane:

$$\langle \psi | U_c | \vec{q} nm \rangle = -2 \int d^2\rho dz_e dz_h \times \frac{[f(\vec{\rho})\phi_0^e(z_e)\phi_0^h(z_h)]^* e^{-i\vec{q}\vec{\rho}} \phi_n^e(z_e)\phi_m^h(z_h)}{\sqrt{|\vec{\rho}|^2+(z_e-z_h)^2}}. \quad (6)$$

The perturbative contribution to the binding energy δE_x is given by a sum over the continuum of states with excitation energy $\Delta_{nm}=\epsilon_n^e-\epsilon_0^e+\epsilon_m^h-\epsilon_0^h$:

$$\delta E_x = \sum_{n,m\neq 0,0} \frac{1}{4\pi^2} \int d^2q \frac{|\langle \psi | U_c | \vec{q} nm \rangle|^2}{q^2+\Delta_{nm}+E_x}. \quad (7)$$

We determine the binding energy E_x and relative wave function $f(\vec{\rho})$ within the quasi-two-dimensional approximation by a numerical solution of Eq. (3) for an $Al_{0.4}Ga_{0.6}As/GaAs$ quantum well.[15,16] Figure 5 shows the relative correction $\delta E_x/E_x$ and the binding energy as a function of the width w of the well. The binding energy has a broad maximum for a width of approximately 5 ML in agreement with the variational calculations of Ref. 12. The perturbative correction remains very small for widths ranging from 5 to 15 ML although the confining potential has a single bound state. For smaller widths, however, δE_x sharply rises with decreasing width and the quasi-two-dimensional approximation is no more accurate due to the substantial leak of the wave functions into the barrier region.

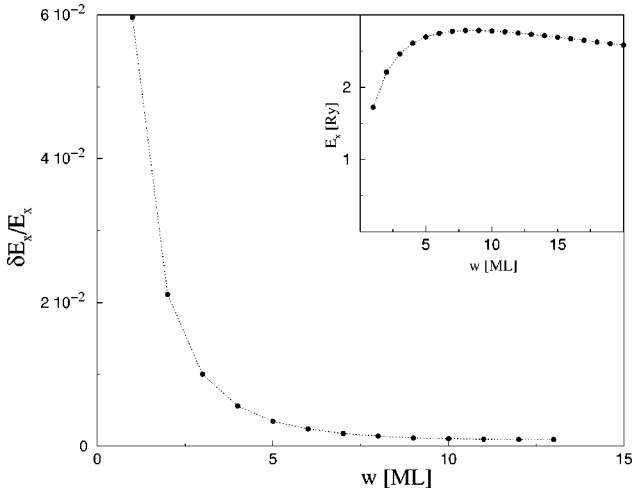

FIG. 5. Relative correction to the exciton binding energy $\delta E_x/E_x$ as a function of width w of the well in monolayers. The correction computed by including perturbatively unconfined states in the transverse direction remains very small for widths larger than 5 but sharply increases for smaller widths. The inset shows the binding energy within the quasi-two-dimensional approximation.

IV. DISORDER AND RANDOM POTENTIAL

This section discusses the model of width fluctuations and the resulting potential for the exciton. It shows that both the correlation length and the strength of the random potential depend on the ratio of island size to exciton radius.

In $GaAs/Al_xGa_{1-x}As$ one of the interface remains rough on the scale of the exciton radius while much larger islands can form on the other interface upon growth interruption. We focus here on the splitting of the excitonic line due to the presence of large islands and therefore consider only the disorder at the smooth interface and width fluctuations of one monolayer.

The disorder consists of random configurations of islands with various shapes and sizes. The present model avoids any arbitrary choice of shape that can introduce artificial structures in the spectrum. For instance a distribution of islands generated by square plaquettes of fixed size ξ gives unphysical peaks, which correspond to particular geometrical arrangements of several plaquettes into a larger island. Here a continuous distribution of shapes and of sizes is achieved by generating islands via a continuous Gaussian field as described below.

The width fluctuations $\delta w(\vec{r})$ in units of the monolayer height are described by a discrete random field with value 0,1. We omit the thinner width with $\delta w=-1$, which gives rise to exciton states with larger confining energies. The discrete variable δw is generated by a continuous Gaussian field $u(\vec{r})$ via the relation $\delta w(\vec{r})=\Theta[U-u(\vec{r})]$ as explained in Appendix A.[17] A distribution of islands with averaged density n and with typical size ξ is obtained by imposing both the mean value $\langle \delta w \rangle = n$ and an exponential correlation of δw with distance:

$$\langle \delta w(\vec{r}) \delta w(\vec{r}') \rangle - n^2 = n(1-n)\exp\left(-\frac{|\vec{r}-\vec{r}'|}{\xi}\right). \quad (8)$$

The inset of Fig. 6 shows a typical disorder configuration, which consists of smooth islands with different shapes and sizes. The density of islands $n=0.3$ is large enough so that neighboring islands may coalesce into conglomerates whose sizes exceed the typical size ξ as indicated by the arrow on the figure. In order to have a feeling of the distribution of islands for various densities, we plot in Fig. 6 the probability

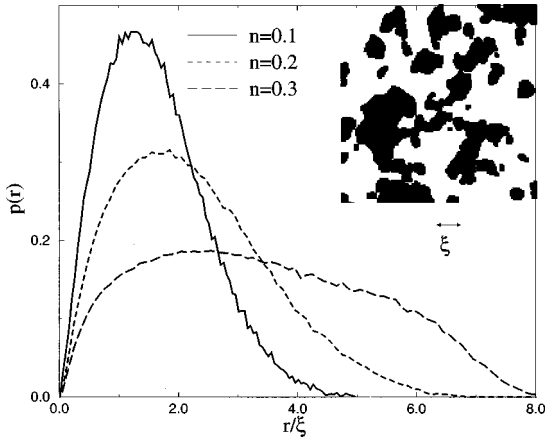

FIG. 6. Probability distribution of island sizes $p(r)$ as a function of radius of the island in units of the typical size ξ for different densities n. The continuous distribution broadens with increasing density due to the coalescence of neighboring islands. The inset shows a configuration of islands for $n=0.3$ with ξ indicated by the double arrow.

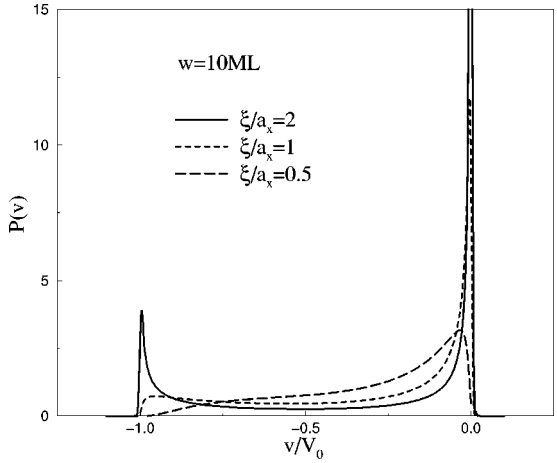

FIG. 7. Distribution $P(v)$ of the random potential as a function of normalized potential strength v/V_0 and for different ratios of island size ξ to exciton radius a_x for a well of 10 ML. Logarithmic singularities gradually build up at the edge of the spectrum $v/V_0=0$ and -1.

distribution $p(r)$ that a position chosen randomly belongs to an island of radius r, namely the product of the density of islands with radius r and of the area of the island. The whole distribution scales with the typical size ξ. While at low density $p(r)$ is peaked around $r=\xi$ the distribution broadens with increasing density since neighboring islands tend to coalesce. However for all densities the distribution has a well-defined maximum that scales with the typical island size ξ. The numerical results in the rest of the paper are obtained for a density $n=0.3$.

The potential $V(\vec{R})$ in Eq. (4) is a convolution of the width fluctuations δw and of the exciton relative wave function, which is taken for simplicity as an exponential $f(\vec{\rho}) \propto \exp(-|\vec{\rho}|/a_x)$ where the exciton radius is computed from the solution of Eq. (2). The random potential depends on two length scales, namely the typical island size ξ via the correlations of δw and the exciton radius a_x via f. The amplitude of the potential varies for wells of different widths w since both V_e and V_h depend on w. However, the ratio V_e/V_h is insensitive to the width and the random-potential scales with the total amplitude $V_0=V_e+V_h$.

The rest of the section studies the statistical properties of the potential for different island sizes ξ in terms of the correlation length and of the potential distribution $P(v)$ averaged over the volume Ω: $P(v)=\int d^2R\langle\delta[v-V(\vec{R})]\rangle/\Omega$. The correlation length is shown to vary from a_x in the small island regime to ξ for large islands. The potential distribution has a single peak for $\xi \ll a_x$, which splits into a doublet with increasing island size.

A. Large-island regime

The potential is proportional to the width fluctuations: $V(\vec{R}) \simeq -V_0 \delta w(\vec{R})$. It varies abruptly at the island edges and has the full amplitude V_0. The potential distribution consists of two δ functions at the energies 0 and $-V_0$ with weights $1-n$ and n, respectively. The potential is exponentially correlated over the distance ξ as the width fluctuations.

B. Small-island regime

The potential has a Gaussian distribution derived in Appendix B and a reduced amplitude[10] $\langle V(\vec{R})^2\rangle \propto (\xi/a_x)^2$. At large distance the potential is exponentially correlated over the distance $m_h a_x/M$. However, for excitonic states localized over a distance much larger than this length scale, the potential can be considered as a white-noise potential with an amplitude Γ that does not depend on a_x anymore:

$$\langle V(\vec{R})V(0)\rangle-(nV_0)^2=2\pi\xi^2 n(1-n)V_0^2\delta(\vec{R})=\Gamma\delta(\vec{R}). \tag{9}$$

In the next section we will show numerical evidence that a model with white-noise potential gives a correct description of the absorption spectrum in the small-island regime.

C. Intermediate regime

The potential distribution $P(v)$ is evaluated numerically for a finite system by sampling several random configurations of the interface disorder. The distribution is constructed from its Chebyshev moments using the kernel polynomial method of Silver *et al.*[18,19]

Figure 7 shows the potential distribution $P(v)$ as a function of the normalized strength v/V_0 for several ratios ξ/a_x. The distribution $P(v)$ shows with increasing island size a weak bump appearing on the low-energy side, which gradually moves towards the edge of the spectrum. The bump is much weaker than the main peak because of the small density of islands. For $\xi \gg a_x$ the potential varies very rapidly through the edges of islands and approaches exponentially the value $-V_0$ or 0 when moving away from the edges. This exponential behavior gives rise to logarithmic singularities at both $v/V_0=0$ and -1 as illustrated in Fig. 7.

V. ABSORPTION SPECTRUM

The calculations of the absorption spectrum $\alpha(E)$ use the same numerical method as for the potential distribution. We show numerical evidence that the spectrum depends mostly

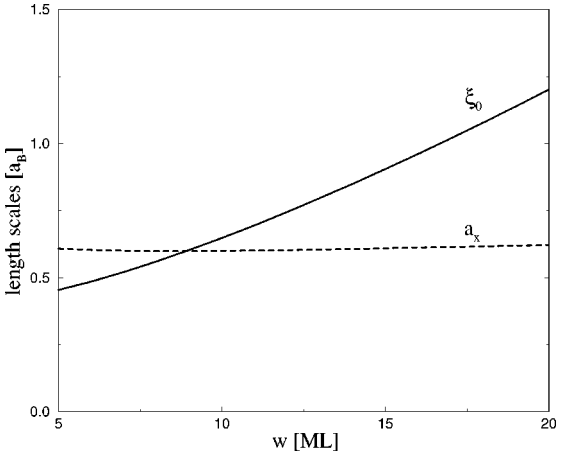

FIG. 8. Localization length ξ_0 and exciton radius a_x in units of the effective Bohr radius a_B as a function of the width w of the $GaAs/Al_{0.4}Ga_{0.6}As$ well. The localization length increases rapidly with w due to the strong dependence of V_0 on width while the exciton radius remains nearly constant in the whole range of w.

on ξ/ξ_0 by comparing the results for various widths w in the range $5 \leqslant w \leqslant 20$ where the splitting of the excitonic peak was experimentally observered.[1,6] In this range the localization length varies by a factor of 2 while the exciton radius remains nearly constant as shown in Fig. 8.

In the small-island regime $\xi \ll \xi_0$, the numerical results compare well to analytical calculations for a white-noise potential except for the position of the exciton peak, which still depends on the correlation length of the disorder. In the large-island regime $\xi \gg \xi_0$, the absorption spectrum shows a splitting of the exciton peak into a doublet. The localization properties of the states are analyzed at the end of the section.

A. Small-island regime

Figure 4 shows the absorption spectrum $\alpha(E)$ as a function of E/V_0 for $\xi/\xi_0 = 1/4$ and different widths of the well. The different curves have a very similar shape and width while they slightly differ in the position of the maximum and in the peak value. The spectrum is asymmetric with a long tail at high energy while it vanishes exponentially fast on the low-energy side.

Comparison in Fig. 4 of the numerical results with the analytic formula of Ref. 11 for a white-noise potential reveals that while both have a similar asymmetric shape, the analytic formula fails to properly position its peak or to yield physically realistic high-energy tail.[20]

The analytic approach is only valid for a δ-correlated potential. The inclusion of the exact correlation function, however, will change the high-energy tail:

$$\alpha(E) \propto \frac{1}{E^2}\left\{ \frac{V_e}{V_0(1+m_h E/4E_x m_e)^{3/2}} + \frac{V_h}{V_0(1+m_e E/4E_x m_h)^{3/2}} \right\}^2 . \qquad (10)$$

The correction of the high-energy tail allows the new analytic curve shown as dots in Fig. 4 to obtain the correct average energy and hence to agree with the numerical results.

The spectrum for a purely white-noise potential depends only on the strength $\Gamma \propto V_0(\xi/\xi_0)^2$ in Eq. (9) and therefore exactly scales with E/V_0 and ξ/ξ_0. The deviation from the scaling for different widths w may be attributed to the correlations of the random potential which depend on the exciton radius a_x as well.

B. Intermediate regime

Figure 2 shows the absorption spectrum for different widths and ratios ξ/ξ_0 in the transition regime where the exciton peak starts to split. The splitting of the excitonic peak is governed essentially by the ratio ξ/ξ_0 since the curves for different widths w but a given ξ/ξ_0 almost coincide.

Figure 3 shows the exciton peak splitting as the island size ξ increases through a narrow range $\xi_0/4 < \xi < 2\xi_0$. The single asymmetric peak for $\xi = \xi_0/4$ broadens with increasing island size until it splits at $\xi = \xi_0$. The weak bump at low energy, which first appears for $\xi = \xi_0$, gradually sharpens and moves towards the edge of the spectrum as ξ approaches $2\xi_0$.

C. Localization properties

We show now that for large islands $\xi > \xi_0$ the states, which contribute to the low-energy peak are localized within a single island while states at higher energy extend over many different islands.

We compute the normalized local density of states $d(E)$ defined as the ratio of density of states within islands to total density of states:

$$d(E) = \frac{\int d^2R\, \delta w(\vec{R}) \left\langle \sum_n |\kappa_n(\vec{R})|^2 \delta(E-E_n) \right\rangle}{\int d^2R \left\langle \sum_n |\kappa_n(\vec{R})|^2 \delta(E-E_n) \right\rangle} . \qquad (11)$$

Figure 9 displays $d(E)$ for the well of 20 ML in the large-island regime $\xi = 2\xi_0$ where the exciton peak has already split. At high energy, the states extend over many islands and $d(E)$ equals the density of islands $n = 0.3$. At negative energies however $d(E)$ sharply rises with decreasing energy and reaches asymptotically the value 1, which correspond to states confined within an island.

The states that contribute to the two exciton peaks have therefore very different localization properties. At low energy, the spectrum is made out of bound states of single islands while higher energy states are localized by the disorder with a localization radius much larger than the mean distance between islands.

VI. CONCLUSIONS AND DISCUSSION

The presence of interfacial roughness strongly affects the absorption spectrum of narrow quantum wells, which shows a splitting of the exciton peak for sufficiently large islands.

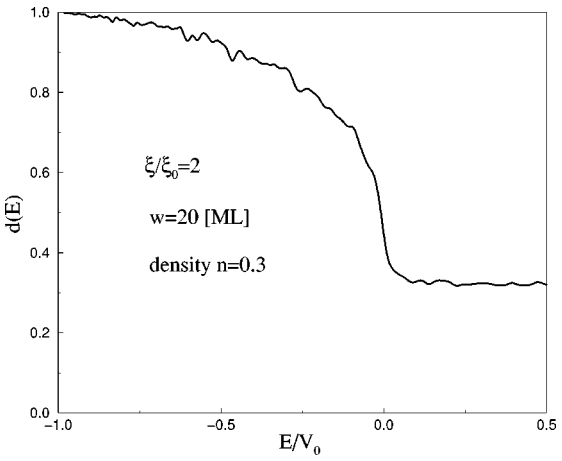

FIG. 9. Normalized local density of states within islands $d(E)$ as a function of normalized energy E/V_0 for $\xi/\xi_0=2$ and for a density of islands $n=0.3$. At low energy, most states are confined within islands while for $E>0$ the states extend over many islands and $d(E)\simeq n$.

We review the main outcomes of this paper and discuss their relevance for experiments.

(1) The exciton center of mass feels a random potential due to the interface roughness whose strength and correlation length depend on the ratio of the typical island size ξ to the exciton radius a_x.

(2) For the absorption spectrum however, the localization length ξ_0 is the important length scale since the spectrum depends mostly on the ratio ξ/ξ_0 and only weakly on the well width w.

(3) The exciton peak in the absorption spectrum gradually splits when the island size reaches ξ_0. This result contrasts with the usual interpretation of experiments, which attributes the splitting to islands of size larger than the exciton radius.[1,6] The two length scales a_x and ξ_0 however have comparable magnitudes in narrow GaAs/Al_xGa_{1-x}As quantum wells as shown in Fig. 8.

Our results suggest that a gradual splitting could be experimentally observed in photoluminescence if the tuning of growth parameters allows the control of island size at the interface. A prediction of the photoluminescence line shape is however beyond the scope of the present paper since it requires the simulation of the thermalization process.[21]

(4) When the island size exceeds the localization length ξ_0, the exciton states at low energy are bound states of a single island while the states at higher energy still extend over many islands. This result is consistent with recent near-field photoluminescence experiments, which have shown very sharp resonances attributed to quantum-dot states at low energy and a dense set of states at high energy.[14]

ACKNOWLEDGMENTS

We would like to thank R. Zimmermann, E. Runge, F. Grosse, A. L. Efros, and R. Sooryakumar for very useful discussions and suggestions. This work was supported at Ohio State University by the Swiss National Science Foundation and the US DOE-Basic Energy Sciences, Division of Material Sciences, and at the Max Planck Institute by the Max Planck Society.

APPENDIX A

The random variable $\delta w(\vec{r})$ that describes the width fluctuations takes only discrete values $\delta w=0,1$ and has long-range correlations. Following Ref. 17, the appendix presents the procedure that generates random configurations of δw with any given correlation function $g(\vec{r})=\langle \delta w(\vec{r})\,\delta w(0)\rangle - n^2$.

The procedure relies on the discretization of a Gaussian continuous field $u(\vec{r})$, which can be easily generated for any correlation function $\sigma(\vec{r})$: $\delta w(\vec{r})=\Theta[U-u(\vec{r})]$. The average value for the discrete field $\langle \delta w\rangle = n$ and its correlation function $g(\vec{r})$ depend on $\sigma(\vec{r})$ and on the parameter U:

$$n=\frac{1}{\sqrt{2\pi}}\int_{-\infty}^{U} e^{-x^2/2}dx, \tag{A1}$$

$$g(\vec{r})=\int_0^{\sigma(\vec{r})/\sigma(0)} \frac{e^{-U^2/(1+x)}}{\sqrt{1-x^2}}\,\frac{dx}{2\pi}. \tag{A2}$$

Inverting the previous equations relates σ and U to any desired $g(\vec{r})$ and n. At large distances both g and σ decay with the same functional dependence. At smaller distance however the correlation functions differ. For an exponential $g(\vec{r})$, the function $\sigma(\vec{r})$ has a Gaussian shape at small distances.

APPENDIX B

We give a derivation of the distribution $P(v)$ in the regime of small islands $\xi \ll a_x$, which is based on an expansion in cumulant averages $\mu_k=\langle [V(\vec{R})]^k\rangle_c$ of the random potential:[22]

$$P(v)=\langle \delta[v-V(\vec{R})]\rangle=\int_{-\infty}^{\infty} e^{iv\lambda}\exp\left[\sum_{k=1}^{\infty}\frac{(-i\lambda)^k}{k!}\mu_k\right]\frac{d\lambda}{2\pi}. \tag{B1}$$

Since the random potential in Eq. (4) is a convolution of the width fluctuations δw and of the exciton relative wave function the cumulant averages μ_k involve the products of $\delta w(\vec{r})$ at different positions $\vec{r}$:

$$\mu_k=\int d^2r_1\cdots d^2r_k F(\vec{r}_1)\cdots F(\vec{r}_k)\langle \delta w(\vec{r}_1)\cdots\delta w(\vec{r}_k)\rangle_c,$$

$$F(\vec{r})=\frac{2}{\pi a_x^2}\left[V_e\left(\frac{M}{m_h}\right)^2 e^{-M|\vec{r}|/a_x m_h}+V_h\left(\frac{M}{m_e}\right)^2 e^{-M|\vec{r}|/a_x m_e}\right]. \tag{B2}$$

On one hand, the cumulant $\langle \delta w(\vec{r}_1)\cdots\delta w(\vec{r}_k)\rangle_c$ has a nonzero contribution only when all its points are within a distance ξ of each other. Indeed any cumulant involving two distant points $|\vec{r}_i-\vec{r}_j|\gg\xi$ vanishes because the width fluctuations $\delta w(\vec{r}_i)$ and $\delta w(\vec{r}_j)$ are statistically uncorrelated.

On the other hand, the function $F(\vec{r})$ varies slowly over a distance $a_x \gg \xi$ and the product of $F(\vec{r}_1)\cdots F(\vec{r}_k)$ in Eq. (B2) is approximated by $F(\vec{r}_1)^k$ due to the locality of the cumulant.

Finally, the cumulants μ_k rapidly decreases with the order k as $(\xi/a_x)^{2k-2}$ in the limit $a_x \gg \xi$. In particular the second-order cumulants reads

$$\mu_2 = \frac{n(1-n)}{2\pi}\left(\frac{\xi}{a_x}\right)^2\left[\left(\frac{V_e M}{m_h}\right)^2 + 8V_eV_h + \left(\frac{V_h M}{m_e}\right)^2\right]. \tag{B3}$$

In the small-island regime the first- and second-order cumulant dominate the expansion (B1) and the potential distribution is a Gaussian of width μ_2 centered around $\mu_1 = n(V_e + V_h)$.

[1] E. S. Koteles, B. S. Elman, C. Jagannath, and Y. J. Chen, Appl. Phys. Lett. **49**, 1465 (1986); D. Bimberg, D. Mars, J. N. Miller, R. Bauer, and D. Oertel, J. Vac. Sci. Technol. B **4**, 1014 (1986).

[2] H. Sakaki, M. Tanaka, and J. Yoshino, Jpn. J. Appl. Phys., Part 2 **24**, L417 (1985).

[3] F. Grosse and R. Zimmermann, Superlattices Microstruct. **17**, 439 (1995).

[4] A. Ourmazd, D. W. Taylor, J. Cunningham, and C. W. Tu, Phys. Rev. Lett. **62**, 933 (1989).

[5] J. Christen, M. Grundmann, and D. Bimberg, Appl. Surf. Sci. **41/42**, 329 (1989).

[6] For a review see M. A. Herman, D. Bimberg, and J. Christen, J. Appl. Phys. **70**, R1 (1991).

[7] S. Subramanian, J. J. Lih, R. Sooryakumar, T. L. Gustafson, E. Koteles, and R. Elman (unpublished).

[8] D. S. Citrin, Phys. Rev. B **54**, 14 572 (1996); S. Haacke, R. A. Taylor, R. Zimmermann, I. Bar-Joseph, and B. Deveaud, Phys. Rev. Lett. **78**, 2228 (1997).

[9] S. D. Baranovskii and A. L. Efros, Fiz. Tekh. Poluprovodn. **12**, 2233 (1978) [Sov. Phys. Semicond. **12**, 1328 (1978)].

[10] R. Zimmermann, Phys. Status Solidi B **173**, 129 (1992); R. Zimmermann and E. Runge, J. Lumin. **60**, 320 (1994).

[11] Al. L. Efros, C. Wetzel, and J. M. Worlock, Phys. Rev. B **52**, 8384 (1995); M. E. Raikh and Al. L. Efros, Fiz. Tverd. Tela (Leningrad) **26**, 106 (1984) [Sov. Phys. Solid State **26**, 61 (1984)].

[12] J. Christen and D. Bimberg, Phys. Rev. B **42**, 7213 (1990).

[13] M. Grundmann and D. Bimberg, Phys. Rev. B **38**, 13 486 (1988); B. Zhu and K. Huang, *ibid.* **36**, 8102 (1987).

[14] D. Gammon, E. S. Snow, B. V. Shanabrook, D. S. Katzer, and D. Park, Phys. Rev. Lett. **76**, 3005 (1996).

[15] The conduction- and valence-band offsets and effective masses are taken from Ref. 13 except for the masses in the barrier region where we use the same values as in the well.

[16] The sum in Eq. (7) is restricted to the single-particle excitations with $n \neq 0, m = 0$ or $n = 0, m \neq 0$, which contribute to more than 95% of δE_x.

[17] H. Tomita, in *Formation Dynamics and Statistics of Patterns*, edited by K. Kawasaki, M. Suzuki, and A. Onuki (World Scientific, Singapore, 1990), Vol. I.

[18] R. N. Silver, H. Roeder, A. F. Voter, and J. D. Kress, J. Comp. Physiol. **124**, 115 (1996).

[19] The results presented here have been obtained for 1500 Chebyshev moments, 2000 random configurations, and a sample of lateral size $750 a_B$.

[20] B. I. Halperin and M. Lax, Phys. Rev. **153**, 802 (1967); D. J. Thouless and M. E. Elzain, J. Phys. C **11**, 3425 (1978).

[21] R. Zimmermann and E. Runge, Phys. Status Solidi A **164**, 511 (1997); R. Zimmermann, F. Grosse, and E. Runge, Pure Appl. Chem. **69**, 1179 (1997).

[22] R. Kubo, J. Phys. Soc. Jpn. **17**, 1100 (1962).